

pubs.acs.org/NanoLett Letter

DNA Origami Guided Self-Assembly of Plasmonic Polymers with Robust Long-Range Plasmonic Resonance

Pengfei Wang,*, $^{\vee}$ Ji-Hyeok Huh, $^{\vee}$ Haedong Park, Donglei Yang, Yingwei Zhang, Yunlong Zhang, Jaewon Lee, Seungwoo Lee,* and Yonggang Ke*



Cite This: https://dx.doi.org/10.1021/acs.nanolett.0c04055



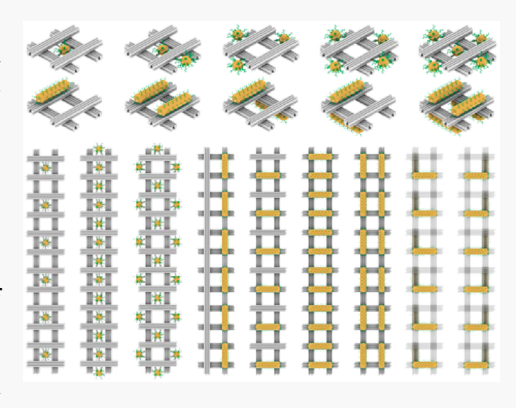
ACCESS

Metrics & More



SI Supporting Information

ABSTRACT: Plasmonic polymers consisting of metallic nanoparticles (NPs) are able to squeeze light into the deep-subwavelength space and transfer along a highly confined nanoscale path in long range. DNA nanotechnology, particularly benefiting from the molecular programmability of DNA origami, has provided otherwise nearly impossible platforms for constructing plasmonic nanoparticle polymers with designer configurations and nanoscale gaps. Here, we design and assemble a DNA origami hashtag tile that is able to polymerize into one-dimensional chains with high rigidity. The DNA origami hashtag chains are used as frames to enable robust, versatile, and precise arrangement of metallic NPs into micrometer-long chiral and magnetic plasmonic polymers, which are capable of efficiently transporting plasmonic angular momentum and magnetic surface plasmonic polaritons at the deep-subwavelength scale. Our work provides a molecular platform for the fabrication of long, straight, and structurally complex nanoparticle polymers with emerging plasmonic properties that are appealing to a variety of fields.



KEYWORDS: Plasmonic polymers, DNA origami, Metallic nanoparticles, Optical Chirality, Magnetic plasmons

NA nanotechnology represents a powerful technique for a variety of custom nanofabrications. 1-3 Particularly, the precise organization of metallic nanoparticles (NPs) by DNA origami has significantly advanced the field of plasmonics and metamaterials.^{4,5} For example, organizing metallic NPs into one-dimensional (1D) architectures of designer configurations, benefiting from excellent programmability of DNA origami, enables the production of plasmonic polymers with emerging optical properties: the linearized gold NP polymers in selfaligned fashion can act as a deep-subwavelength plasmonic waveguide, 6,7 while the helical arrangement of gold NPs along 1D chains provides a platform for chiral plasmonics. 8-10 For NPs' assembly on DNA origami, linear DNA origami helix bundles (HBs) with various cross-sectional geometries have been frequently used for organizing NPs into chains. 6-8 Recently, Liu and colleagues reported V-shaped DNA origami polymers for the dynamic organization of gold nanorods forming reconfigurable plasmonic chiral chains. 10 We also reported the assembly of a plasmonic polymer of NP rings by using a DNA origami hexagon tile. 11 Some other reports employed an alternative strategy by using DNA origami structures as adaptors to induce the hierarchical assembly of metallic NPs to form 1D architectures. 12-14 Nevertheless, limited success in fabricating long, straight, and structurally complex plasmonic polymers has been achieved so far due to the lack of DNA origami frames to allow robust and versatile

organization of NPs forming highly persistent chainlike assemblies, which largely impedes the versatility and plasmonic properties of plasmonic polymers that can be fabricated.

Herein, we aimed to design and assemble a rigid and versatile DNA origami tile, which can be polymerized into rigid 1D chains serving as robust frames for NP assembly. DNA origami hexagon tile is a wireframe-like template that is highly versatile for assembling NPs into structurally complex architectures, but it lacks rigidity to enable the assembly of robust 1D chains. The new DNA origami tile reported here is constituted by orthogonal stacks of two decks, denoted as a hashtag tile, given it structurally resembles a hashtag symbol. It retains the wireframe design of a hexagon tile but with significantly enhanced rigidity attributed to its geometry of orthogonally stacked two decks. Phononic band calculation reveals that the polymerized 1D chain of hashtag tile exhibits significantly higher bending stiffness than that of hexagon tiles by at least one order of magnitude. The optimized assembling conditions for the hashtag tiles and its subsequent linear

Received: October 12, 2020 Revised: November 9, 2020



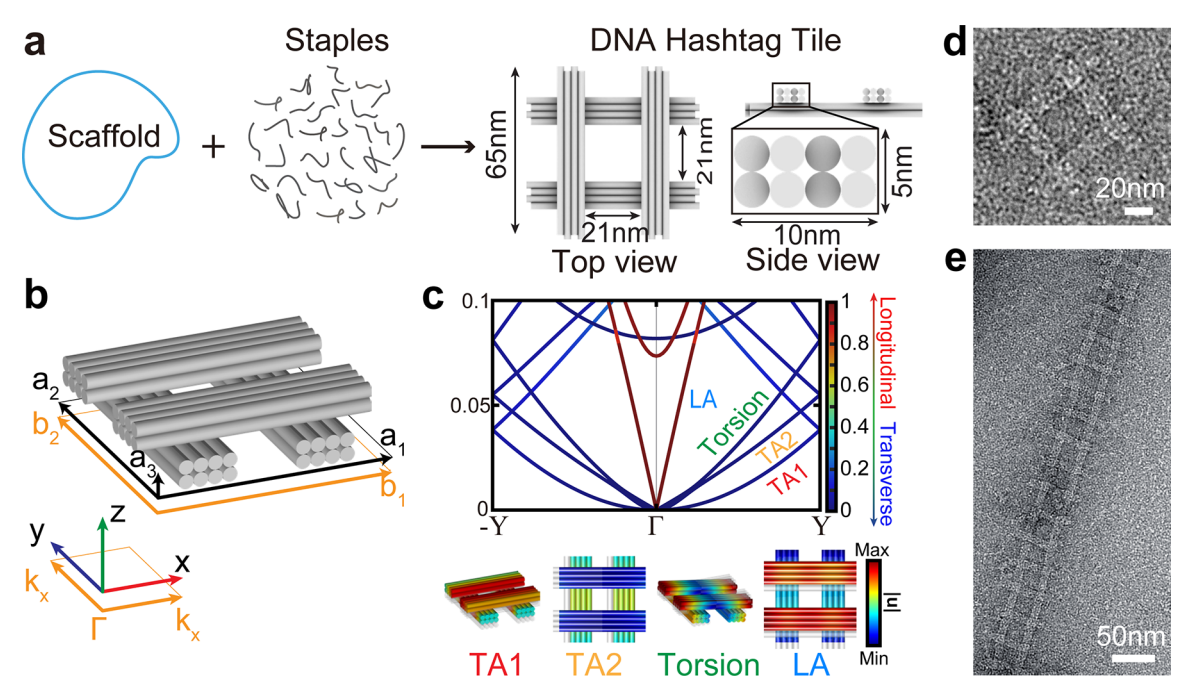


Figure 1. Design, numerical calculations, and assembly of DNA origami hashtag tile polymers. (a) Schematic of DNA origami hashtag tile design and assembly. (b) Unit cell (black outlines) and first Brillouin zone (orange outlines) of hashtag polymer. (c) The numerically calculated phononic band structures (top panels) of the hashtag tile polymer. The corresponding phononic modes are summarized in the bottom panel, where **u** is displacement vector as the eigenstate of the band structures. (d,e) Transmission electron microscopy images of DNA origami hashtag tile monomer and polymers, respectively.

polymerization enable the platforms for the precise organization of chiral and magnetic plasmonic polymers in a strikingly long and straight fashion (Figure S1). The collective set of (i) design principles, (ii) robust folding and polymer assembly, and (iii) plasmonic characterizations were synergistically outlined in this work and will be of general interest not only for the hierarchical organization of DNA origami but also for facilitating the soft DNA approaches to the plasmonic-based nanophotonic applications.

The DNA origami hashtag tile was designed to have four structurally identical decks (2 helices tall, 4 helices wide, 192 bp long) that are orthogonally stacked via scaffold DNA linkage (Figure 1a, Figures S2, S3). The deck is 65 nm long, 10 nm wide, and 5 nm tall, assuming the helical pitch and diameter of B-form DNA is 0.34 nm/bp and 2.5 nm, respectively. The internal square resides at the center of the hashtag tile and has a side length of 21 nm. Connector strands were designed to bridge the ends of designated decks to induce unidirectional hierarchical assembly to form hashtag polymers. Numerical calculations of photonic band structure were performed to compare the mechanical properties of the DNA origami hashtag polymer (Figure 1b,c) and hexagon polymers (Figure S4). Figure 1b illustrates the unit cell (black outlines) and first Brillouin zone (orange outlines) of the hashtag tile polymers. The numerically calculated phononic band structures for the hashtag tile unit is presented in the top panel of Figure 1c. Polymers of hashtag tiles, which are assumed to be dispersed in a buffer solution, can incur four different phononic vibrations including longitudinal mode (denoted as LA), transverse mode along out-of-plane direction (denoted as TA1), transverse mode along in-plane direction (denoted as TA2), and torsion mode (denoted as Torsion), as shown in the bottom panel of Figure 1c. It is noteworthy that the hashtag tile showed the steeper modal slopes of LA, TA1,

TA2, and Torsion modes (along Γ to Y point) than its hexagon counterpart (Figure S4b), evidencing its significantly higher stiffness. We then quantitated the bending stiffness (D) from these phononic band structures as follows ^{16,17}

$$D = \frac{Eh^3}{12(1 - \nu^2)} \tag{1}$$

where E is the effective Young's modulus, ν is the effective Poisson's ratio, and h is the thickness of the unit cell (the calculation details are given in Materials and Methods in the Supporting Information). It turned out that the D value of the hashtag tile chain can be up to 0.105 pN·nm, which was higher than that of hexagon tile counterpart (0.015 pN·nm) by one order of magnitude.

When the assembled polymers adsorbed onto the substrate, phononic vibrations along out-of-plane directions would be difficult to occur; therefore, in-plane modes such as transverse (T) and longitudinal (L) modes can be only induced (Figure S5). In this case, E rather than D can be used to quantitate the mechanical rigidity of the assembled chain due to the absence of out-of-plane modes. It was revealed that the hashtag tile chain can reach up to the E value of 11 897 Pa, which is much higher than that of the hexagon tile chain (1533 Pa); see steeper modal slopes of T and L modes of the hashtag tile chain than those of the hexagon counterparts (Figure S5). Furthermore, it is important to note that the analyses on the persistence length (P_1) of two chains, which can be considered as an experimental quantitation of mechanical rigidity of polymeric chain, ^{18–20} agreed well with the above theoretical results, as shown in Figure S6 (avg. P_1 of ~4.1 μ m for the hashtag tile chain and avg. P_1 of ~ 470 nm for the hexagon tile chain). The superior mechanical stiffness of the hashtag tile polymer is afforded by the cross double-deck rather than single-deck motifs.

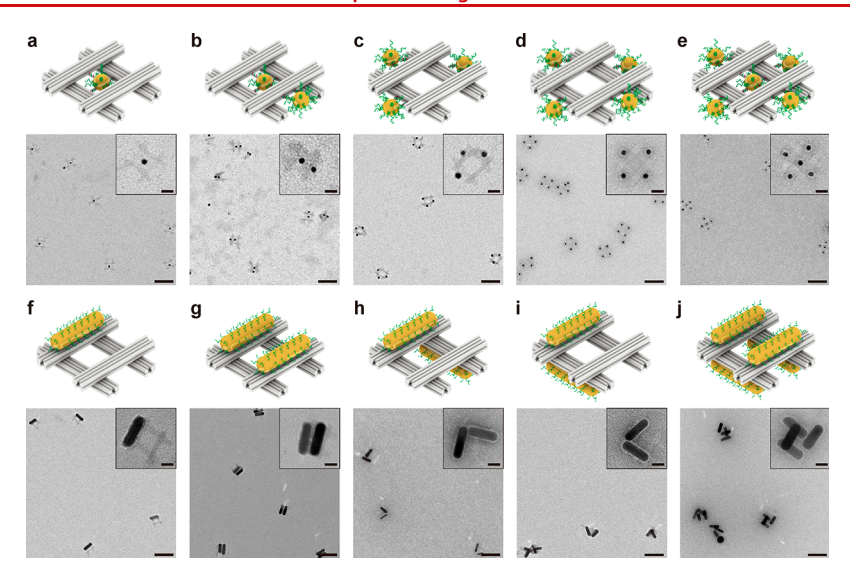


Figure 2. Gold NP clusters on hashtag tile monomers. Assembling gold nanospheres (a-e) and gold nanorods (f-j) onto hashtag tiles at designated locations and with designated numbers. Scale bars: 100 nm, 20 nm (insets).

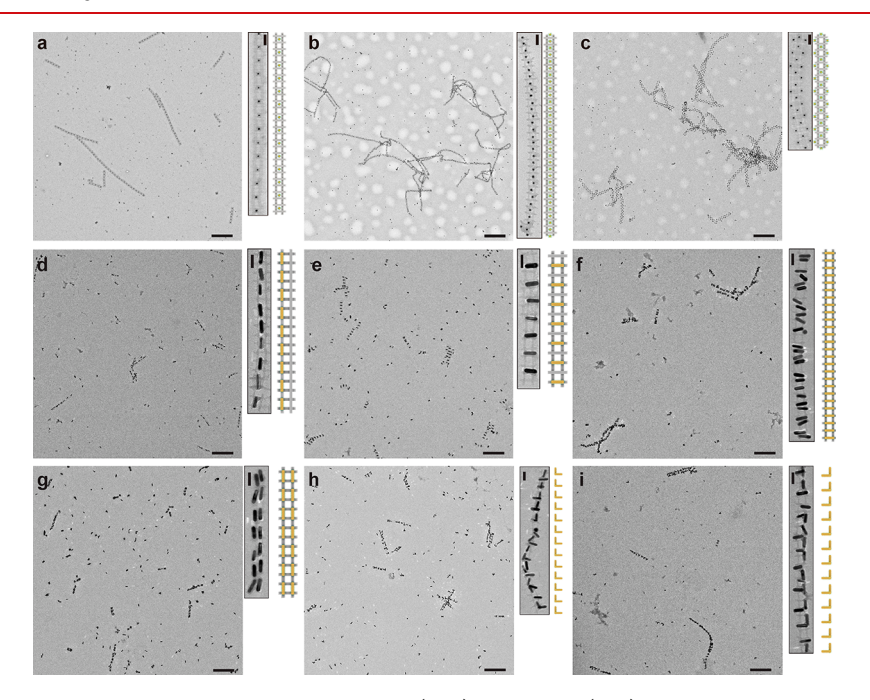


Figure 3. Gold NP polymers on hashtag chains. Assembling AuNSs (a-c) or AuNRs (d-i) onto hashtag chains. Scale bars: 500 nm, 50 nm (insets).

We then examined the assembly of DNA origami hashtag tiles. Transmission electron microscopy (TEM) images of the hashtag tile monomers (Figure 1d) and polymers (Figure 1e) unambiguously confirmed their successful construction with sizes and geometries agreeing to the prescribed designs (Figure S7). The hashtag polymers with length up to several microns were assembled by adding connector strands to induce one-direction hierarchical growth of tiles, suggesting that it has the potential to serve as robust frames to organize metallic NPs forming high-fidelity plasmonic polymers. This long-lasting, 1D chain organization can be attributed to the unique mechanical stiffness of the hashtag tile, as quantitated above.

To precisely assemble gold NPs, staple strands with extended overhangs were placed at designated locations on the hashtag tile forming a total of nine binding sites (Figure S1). One binding site was located within the internal square

(no. 1), four binding sites were on the exterior edges (nos. 2-5), and another four were on the surface of the decks (nos. 6– 9). Each binding site was composed of multiple (2, 4, or 6) single-stranded DNA overhangs protruding from designated staple strands to capture complementary DNA-functionalized NPs via sequence-specific DNA hybridization. The hashtag tile monomers were then used as frames to validate its versatility and capability on assembling gold NPs. We first constructed a group of 10 different gold NP clusters by assembling gold nanospheres (AuNSs, 10 nm in diameter) and gold nanorods (AuNRs, 15 nm in diameter and 40 nm in length) onto the hashtag tiles. The configurations of assemblies were programmed by tuning the number and location of NPs. All NP clusters were successfully assembled as revealed by agarose gel electrophoresis (Figure S8) and unambiguously visualized by TEM (Figure 2, Figures S9-S18). It is worth noting that the

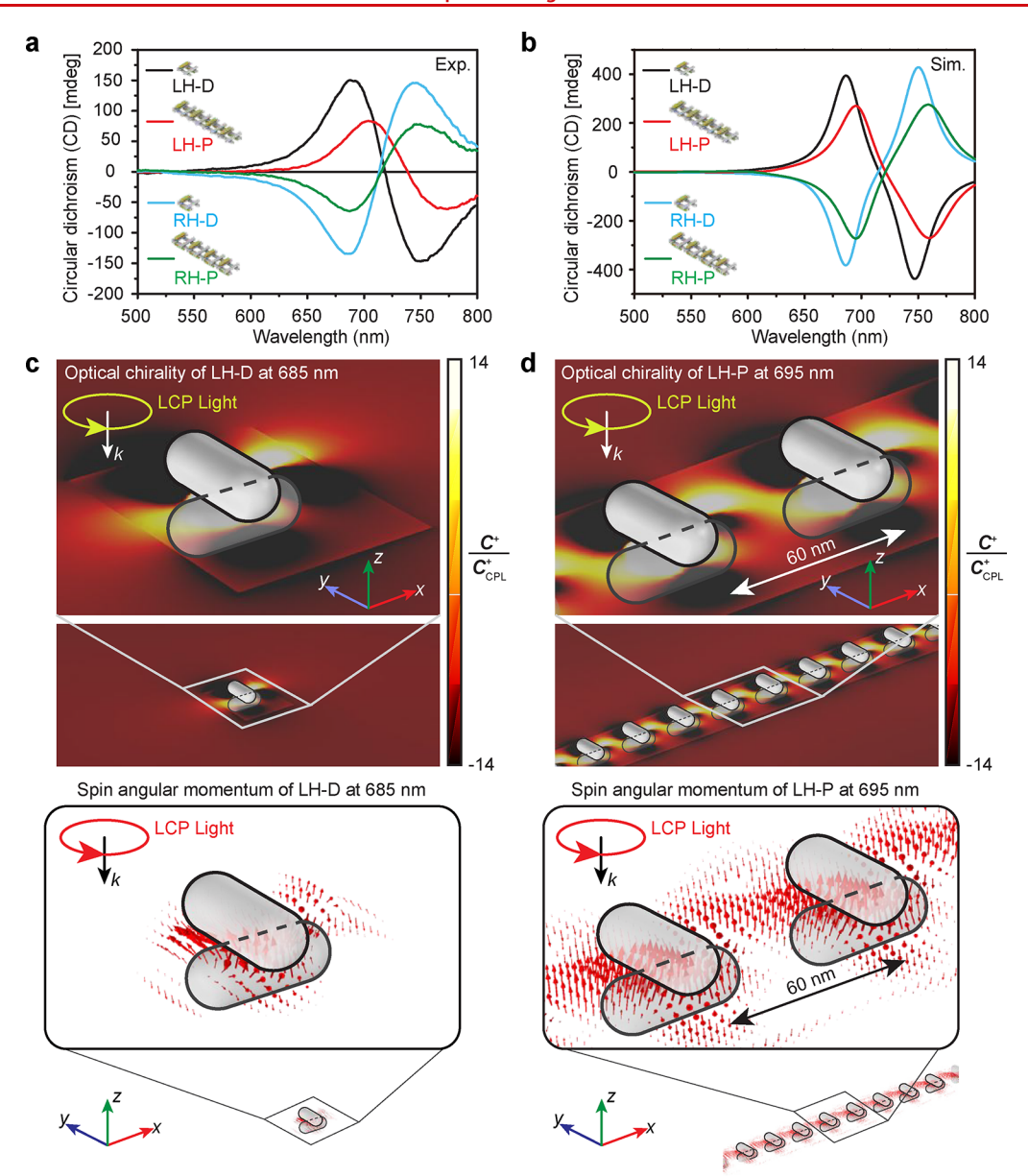


Figure 4. Chiro-optic response of AuNR dimers (LH-D and RH-D) and polymers (LH-P and RH-P). Experimental (a) and numerically calculated (b) CD spectra of chiral AuNR dimers and polymers. Numerically calculated spatial distributions (modal analyses) of optical chirality (top panels) and spin angular momentum (bottom panels) of LH-D (c) and LH-P (d). Herein, the numerical calculations were supported by finite element method (FEM).

cluster composed of four AuNRs (Figure 2j) had a certain degree of dislocation of AuNRs, which may be attributed to the surface drying effect while depositing the clusters on TEM grids. Overall, these NP clusters exhibited prescribed configurations, suggesting the robust and versatile assembling capability of the hashtag tiles.

NP polymers with nine different periodic configurations were constructed on hashtag chain frames, as illustrated in Figure 3. AuNSs (Figure 3a–c, Figures S19–S21) and AuNRs (Figure 3d–i, Figures S22–S27) were anchored onto prescribed locations on the chain frames. TEM imaging revealed the formation of NP polymers with prescribed configurations. Particularly, the NP polymer, shown in Figure 3c, can provide a template for fabricating plasmonic circuits to enable effectively excitation and propagation of a magnetic plasmon (i.e., a magnetic dipolar plasmonic waveguide), which will be experimentally characterized and theoretically calcu-

lated in detail in the following section. Minor defects such as an occasional missing NP in the polymers were observed, especially for complex configurations involving a large number of NPs (e.g. assembly in Figure 3c). However, the magnetic plasmonic waveguide was found to be quite tolerant against such structural defects, especially compared with an electric counterpart.²¹ Furthermore, micrometer-long chiral AuNR polymers with left-handed (LH) or right-handed (RH) chirality were successfully assembled (Figure 3h,i).

Next, the corresponding nano-optical characterizations of these plasmonic polymers were performed both experimentally and theoretically. The circular dichroism (CD) spectra of chiral AuNR dimers (LH-D, RH-D) and polymers (LH-P, RH-P) exhibited characteristic features of the chiro-optic responses (Figure 4a) matching well with the numerical simulations (Figure 4b). Finite element method (FEM), implemented with the appropriate dipolar and chiral descriptions, was used to

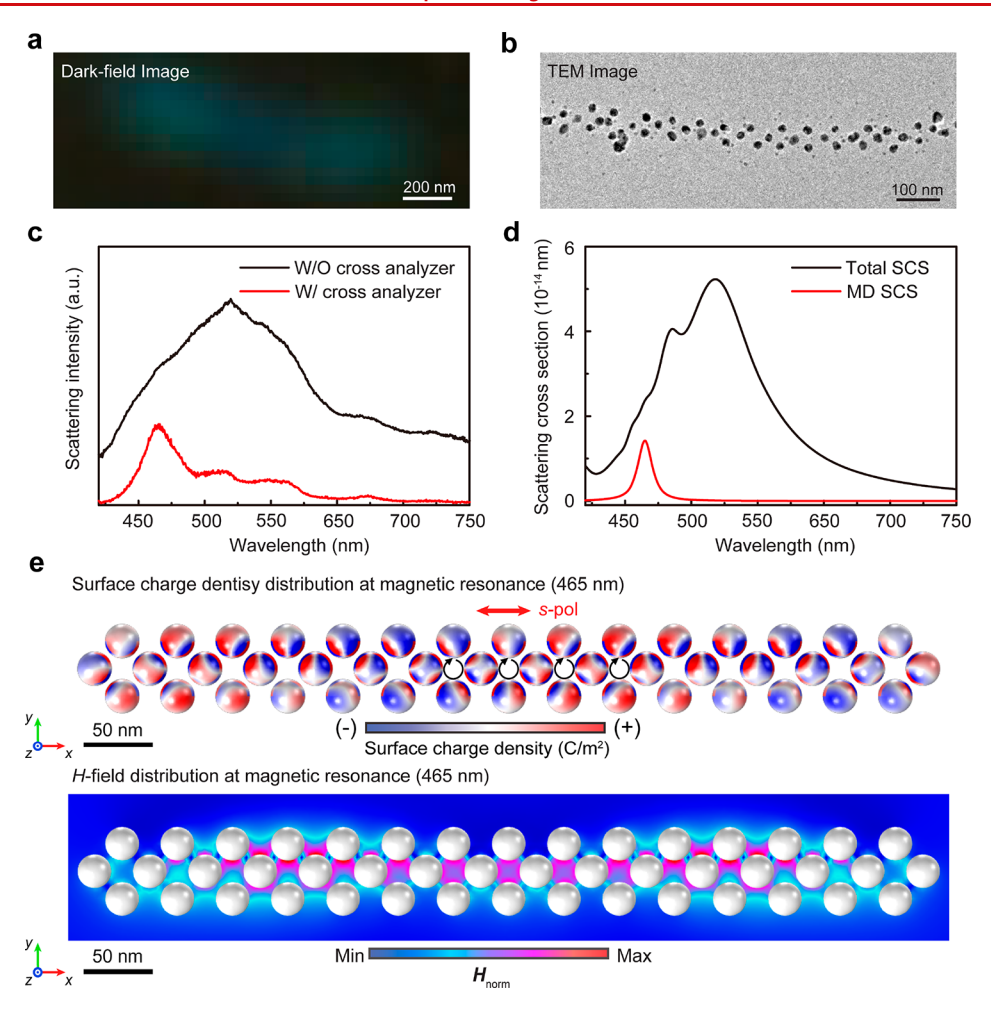


Figure 5. Plasmonic polymers capable of exciting and propagating magnetic dipolar resonance (i.e., magnetic surface plasmon polaritons (SPPs)). (a) Dark-field optical microscope image of the assembled magnetic plasmonic polymers. (b) Corresponding TEM image. (c,d) Dark-field scattering spectra of the scattering image in (a), which were measured with and without cross analyzer, and the corresponding numerical calculation results, respectively. These numerical calculations were performed with FEM. (e) Modal analysis of magnetic SPPs of the plasmonic polymers at the magnetic dipolar resonant wavelength.

theoretically predict the chiro-optic behaviors of the AuNR dimers and polymers. Several features are noteworthy as follows. The AuNR LH-D and RH-D showed distinct chirooptic spectral features, resulting from a highly and strongly confined optical chirality (C) between two AuNRs ($C = \omega/2c^2$ $Im(E^*\cdot H)$, where E and H are complex electric and magnetic fields, and ω is the angular frequency of light). This confined C is directly evidenced by modal analysis of spin angular momentum at plasmonic resonant wavelength (Figure 4c). As a representative example, modal analyses for LH chiral cases (light illumination with left circular polarization (LCP) on LH-D and LH-P) are included in main manuscript, while RH counterparts are summarized in Supporting Information (Figure S28). More strikingly, the resonantly induced C can be coupled between the chiral AuNR dimers and cascaded along the polymer. Corresponding modal analyses, presented in the top panel of Figure 4d, confirmed the coupling of C between the LH-D (or RH-D) in that the hot spot of C can be formed between the LH-D (or RH-D). Corresponding spatial distribution of spin angular momentum further evidenced the coupling of the induced C, as shown in the bottom panel of Figure 4d. This coupling of the induced C gave the origin of redshift on the CD spectra, observed for LH-P (or RH-P). Also, note that during the cascaded propagation of these chiral

oscillations in each AuNR dimer, the dephasing between the radiation from each monomer of chiral AuNR dimer should inevitably give rise to the retardation effect-mediated optical loss.²³ This retardation effect in the chiro-optic response was experimentally evidenced by the dimmed spectral peak and dip of CD features (Figure 4a), agreeing well with the theoretical prediction (Figure 4b).

In addition to chiral polymers, propagation of magnetic plasmons along the AuNS polymers was systematically verified by a synergistic combination of microscopic dark-field scattering spectrum and FEM numerical calculations (Figure 5). Ten nanometers of AuNSs was first anchored on hashtag chain frames (Figure 3c), which then served as precursors to induce in situ silver (Ag) growth to enlarge metallic NPs, while maintaining structural complexity and integrity, leading to the formation of architectures with highly enhanced plasmonic properties. 11,24 Figure 5a,b presents a dark-field optical microscopic image in conjunction with a corresponding TEM image of the fabricated magnetic polymer. The ring inclusions of silver NSs (i.e., plasmonic units enabling excitation of a magnetic dipole²⁵ were found to be assembled into a straight 1D chain (Figure 5b). The bluish scattering line in the dark-field image (Figure 5a) was resulted from the radiation of magnetic surface plasmonic polaritons (SPPs).

The corresponding dark-field scattering spectra with and without the cross analyzer (enabling selective screening of electric dipolar scattering) further evidenced the presence of magnetic SPPs at the wavelengths of 465 nm (Figure 5c), which was in a good agreement with the numerical simulations (Figure 5d). However, additional spectral shoulders with the cross analyzer (at 530, 570, and 650 nm of wavelengths) were observed in contrast to theoretical prediction, because the use of cross analyzer is unable to perfectly screen electric modedriven scattering. As well as the in-plane component, the outof-plane component is generally observed in electrically resonant scattering. Indeed, the remnant scattering intensity resulting from electric dipolar resonance gave an origin of spectral shoulder at 530 nm wavelength, while the rest of two unpredicted peaks at 570 and 650 nm wavelengths resulted from the structural defect-driven electric scattering. The modal analyses at the magnetic resonant wavelength confirmed the excitations of a circulating displacement current and the resultant induction of magnetic field within each ring inclusion of Ag NSs, consequently supporting the distinct presence of the magnetic SPPs to be radiated to far-field (Figure 5e).

In conclusion, we have designed and assembled a generic DNA origami hashtag tile to provide a versatile and deterministic platform for organizing metallic NPs into onedimensional plasmonic polymer architectures, which may be of general interest in the field of self-assembled plasmonic devices. To validate its versatility and generality, we successfully constructed a set of metallic NP architectures with delicate configurations ranging from nanometer-sized clusters to micrometer-sized polymers. Most strikingly, the highly efficient propagations of chiro-optical resonance and magnetic SPPs along the assembled plasmonic polymers were successfully demonstrated both experimentally and theoretically. Furthermore, micrometer-long chiral AuNR polymers were also fabricated on hashtag chain frames. It is worth noting that the hashtag frame is not limited to polymer assemblies. Complex oligomers and two-dimensional arrays may also be assembled to serve as frames for metallic NP organization (Figures S29-S33). Overall, we demonstrated that the DNA origami hashtag tile can be used as pegboards for fabricating plasmonic devices, which hold enormous utilization potentials towards nano-optics.

■ ASSOCIATED CONTENT

5 Supporting Information

The Supporting Information is available free of charge at https://pubs.acs.org/doi/10.1021/acs.nanolett.0c04055.

Materials and methods, additional figures, sequence of DNA strands (PDF)

AUTHOR INFORMATION

Corresponding Authors

Pengfei Wang — Institute of Molecular Medicine, Shanghai Key Laboratory for Nucleic Acid Chemistry and Nanomedicine, State Key Laboratory of Oncogenes and Related Genes, Renji Hospital, School of Medicine, Shanghai Jiao Tong University, Shanghai 200127, China; orcid.org/0000-0002-3125-763X;

Email: pengfei.wang@sjtu.edu.cn

Seungwoo Lee – KU-KIST Graduate School of Converging Science and Technology and Department of Integrative Energy Engineering, Department of Biomicrosystem Technology, and KU Photonics Center, Korea University, Seoul 02841, Republic of Korea; orcid.org/0000-0002-6659-3457; Email: seungwoo@korea.ac.kr

Yonggang Ke — Department of Chemistry, Emory University, Atlanta, Georgia 30322, United States; Wallace H. Coulter Department of Biomedical Engineering, Georgia Institute of Technology and Emory University, Atlanta, Georgia 30322, United States; orcid.org/0000-0003-1673-2153; Email: yonggang.ke@emory.edu

Authors

Ji-Hyeok Huh – KU-KIST Graduate School of Converging Science and Technology, Korea University, Seoul 02841, Republic of Korea

Haedong Park – KU-KIST Graduate School of Converging Science and Technology, Korea University, Seoul 02841, Republic of Korea

Donglei Yang — Institute of Molecular Medicine, Shanghai Key Laboratory for Nucleic Acid Chemistry and Nanomedicine, State Key Laboratory of Oncogenes and Related Genes, Renji Hospital, School of Medicine, Shanghai Jiao Tong University, Shanghai 200127, China

Yingwei Zhang — State Key Laboratory of Chemical Resource Engineering, College of Materials Science and Engineering, Beijing University of Chemical Technology, Beijing 100029, China; orcid.org/0000-0001-8586-864X

Yunlong Zhang – Department of Chemistry, Emory University, Atlanta, Georgia 30322, United States

Jaewon Lee – KU-KIST Graduate School of Converging Science and Technology, Korea University, Seoul 02841, Republic of Korea

Complete contact information is available at: https://pubs.acs.org/10.1021/acs.nanolett.0c04055

Author Contributions

 ${}^{
abla}$ P.W. and J.-H.H. contributed equally to this work.

Notes

The authors declare no competing financial interest.

ACKNOWLEDGMENTS

P.W. thanks the support from the Ministry of Science and Technology of China (2018YFA0902601) and from the National Natural Science Foundation of China (21974086). S.L. thanks the support from the National Research Foundation (NRF) of Korea under Project Number 2017M3D1A1039421 (Future Material Discovery Project), 2019R1A2C2004846 (Midcareer researcher supporting project), 2019R1A4A1028121 (Basic research laboratory project), and the KU-KIST School Project. Y.K. acknowledges the support from the National Science Foundation under Grant ECCS-1807568. P.W. and J.H. contributed equally to this work.

REFERENCES

- (1) Hong, F.; Zhang, F.; Liu, Y.; Yan, H. DNA Origami: Scaffolds for Creating Higher Order Structures. *Chem. Rev.* **2017**, *117* (20), 12584–12640.
- (2) Wang, P. F.; Meyer, T. A.; Pan, V.; Dutta, P. K.; Ke, Y. G. The Beauty and Utility of DNA Origami. *Chem-Us* **2017**, 2 (3), 359–382.
- (3) Seeman, N. C.; Sleiman, H. F. DNA nanotechnology. *Nat. Rev. Mater.* **2018**, 3 (1), 1–23.
- (4) Liu, N.; Liedl, T. DNA-Assembled Advanced Plasmonic Architectures. Chem. Rev. 2018, 118 (6), 3032-3053.

- (5) Lan, X.; Wang, Q. Self-Assembly of Chiral Plasmonic Nanostructures. *Adv. Mater.* **2016**, 28 (47), 10499–10507.
- (6) Gur, F. N.; McPolin, C. P. T.; Raza, S.; Mayer, M.; Roth, D. J.; Steiner, A. M.; Loffler, M.; Fery, A.; Brongersma, M. L.; Zayats, A. V.; Konig, T. A. F.; Schmidt, T. L. DNA-Assembled Plasmonic Waveguides for Nanoscale Light Propagation to a Fluorescent Nanodiamond. *Nano Lett.* **2018**, *18* (11), 7323–7329.
- (7) Gur, F. N.; Schwarz, F. W.; Ye, J. J.; Diez, S.; Schmidt, T. L. Toward Self-Assembled Plasmonic Devices: High-Yield Arrangement of Gold Nanoparticles on DNA Origami Templates. *ACS Nano* **2016**, *10* (5), 5374–5382.
- (8) Kuzyk, A.; Schreiber, R.; Fan, Z. Y.; Pardatscher, G.; Roller, E. M.; Hogele, A.; Simmel, F. C.; Govorov, A. O.; Liedl, T. DNA-based self-assembly of chiral plasmonic nanostructures with tailored optical response. *Nature* **2012**, *483* (7389), 311–314.
- (9) Urban, M. J.; Dutta, P. K.; Wang, P. F.; Duan, X. Y.; Shen, X. B.; Ding, B. Q.; Ke, Y. G.; Liu, N. Plasmonic Toroidal Metamolecules Assembled by DNA Origami. *J. Am. Chem. Soc.* **2016**, *138* (17), 5495–5498.
- (10) Lan, X.; Liu, T.; Wang, Z.; Govorov, A. O.; Yan, H.; Liu, Y. DNA-Guided Plasmonic Helix with Switchable Chirality. *J. Am. Chem. Soc.* **2018**, *140* (37), 11763–11770.
- (11) Wang, P. F.; Huh, J. H.; Lee, J.; Kim, K.; Park, K. J.; Lee, S.; Ke, Y. Magnetic Plasmon Networks Programmed by Molecular Self-Assembly. *Adv. Mater.* **2019**, *31* (29), 1901364.
- (12) Lee, J.; Huh, J.-H.; Kim, K.; Lee, S. DNA Origami-Guided Assembly of the Roundest 60–100 nm Gold Nanospheres into Plasmonic Metamolecules. *Adv. Funct Mater.* **2018**, 29 (15), 1707309.
- (13) Tian, Y.; Wang, T.; Liu, W. Y.; Xin, H. L.; Li, H. L.; Ke, Y. G.; Shih, W. M.; Gang, O. Prescribed nanoparticle cluster architectures and low-dimensional arrays built using octahedral DNA origami frames. *Nat. Nanotechnol.* **2015**, *10* (7), 637–644.
- (14) Lan, X.; Su, Z.; Zhou, Y.; Meyer, T.; Ke, Y.; Wang, Q.; Chiu, W.; Liu, N.; Zou, S.; Yan, H.; Liu, Y. Programmable Supra-Assembly of a DNA Surface Adapter for Tunable Chiral Directional Self-Assembly of Gold Nanorods. *Angew. Chem., Int. Ed.* **2017**, *56* (46), 14632–14636.
- (15) Park, S. H.; Park, H.; Hur, K.; Lee, S. Design of DNA Origami Diamond Photonic Crystals. *ACS Appl. Bio Mater.* **2020**, 3 (1), 747–756.
- (16) Davami, K.; Zhao, L.; Lu, E.; Cortes, J.; Lin, C.; Lilley, D. E.; Purohit, P. K.; Bargatin, I. Ultralight shape-recovering plate mechanical metamaterials. *Nat. Commun.* **2015**, *6*, 10019.
- (17) Pocivavsek, L.; Pugar, J.; O'Dea, R.; Ye, S. H.; Wagner, W.; Tzeng, E.; Velankar, S.; Cerda, E. Topography-driven surface renewal. *Nat. Phys.* **2018**, *14* (9), 948–953.
- (18) Schiffels, D.; Liedl, T.; Fygenson, D. K. Nanoscale structure and microscale stiffness of DNA nanotubes. *ACS Nano* **2013**, 7 (8), 6700–10.
- (19) Yao, G.; Zhang, F.; Wang, F.; Peng, T.; Liu, H.; Poppleton, E.; Sulc, P.; Jiang, S.; Liu, L.; Gong, C.; Jing, X.; Liu, X.; Wang, L.; Liu, Y.; Fan, C.; Yan, H. Meta-DNA structures. *Nat. Chem.* **2020**, *12* (11), 1067–1075.
- (20) Kauert, D. J.; Kurth, T.; Liedl, T.; Seidel, R. Direct mechanical measurements reveal the material properties of three-dimensional DNA origami. *Nano Lett.* **2011**, *11* (12), 5558–63.
- (21) Liu, N.; Mukherjee, S.; Bao, K.; Brown, L. V.; Dorfmuller, J.; Nordlander, P.; Halas, N. J. Magnetic Plasmon Formation and Propagation in Artificial Aromatic Molecules. *Nano Lett.* **2012**, *12* (1), 364–369.
- (22) Tang, Y.; Cohen, A. E. Optical chirality and its interaction with matter. *Phys. Rev. Lett.* **2010**, *104* (16), 163901.
- (23) Ahn, H. Y.; Yoo, S.; Cho, N. H.; Kim, R. M.; Kim, H.; Huh, J. H.; Lee, S.; Nam, K. T. Bioinspired Toolkit Based on Intermolecular Encoder toward Evolutionary 4D Chiral Plasmonic Materials. *Acc. Chem. Res.* **2019**, *52* (10), *2768*–*2783*.
- (24) Zhou, C. Y.; Yang, Y. J.; Li, H. F.; Gao, F.; Song, C. Y.; Yang, D. L.; Xu, F.; Liu, N.; Ke, Y. G.; Su, S.; Wang, P. F. Programming

Surface-Enhanced Raman Scattering of DNA Origami-templated Metamolecules. *Nano Lett.* **2020**, *20* (5), 3155–3159.

(25) Roller, E. M.; Khorashad, L. K.; Fedoruk, M.; Schreiber, R.; Govorov, A. O.; Liedl, T. DNA-Assembled Nanoparticle Rings Exhibit Electric and Magnetic Resonances at Visible Frequencies. *Nano Lett.* **2015**, *15* (2), 1368–1373.